

# Glutathione Depletion Induced by c-Myc Downregulation Triggers Apoptosis on Treatment with Alkylating Agents<sup>1</sup>

Annamaria Biroccio\*, Barbara Benassi\*, Francesco Fiorentino<sup>†</sup> and Gabriella Zupi\*

\*Experimental Chemotherapy Laboratory, Experimental Research Center, Regina Elena Cancer Institute, Rome 00158, Italy; <sup>†</sup>“Genoma” Molecular Genetics Laboratory, Rome 00198, Italy

## Abstract

Here we investigate the mechanism(s) involved in the c-Myc–dependent drug response of melanoma cells. By using three M14-derived c-Myc low-expressing clones, we demonstrate that alkylating agents, cisplatin and melphalan, trigger apoptosis in the c-Myc antisense transfectants, but not in the parental line. On the contrary, topoisomerase inhibitors, adriamycin and camptothecin, induce apoptosis to the same extent regardless of c-Myc expression. Because we previously demonstrated that c-Myc downregulation decreases glutathione (GSH) content, we evaluated the role of GSH in the apoptosis induced by the different drugs. In control cells treated with one of the alkylating agents or the others, GSH depletion achieved by L-buthionine-sulfoximine preincubation opens the apoptotic pathway. The apoptosis proceeded through early Bax relocalization, cytochrome *c* release, and concomitant caspase-9 activation, whereas reactive oxygen species production and alteration of mitochondria membrane potential were late events. That GSH was determining in the c-Myc–dependent drug-induced apoptosis was demonstrated by altering the intracellular GSH content of the c-Myc low-expressing cells up to the level of controls. Indeed, GSH ethyl ester–mediated increase of GSH abrogated apoptosis induced by cisplatin and melphalan by inhibition of Bax/cytochrome *c* redistribution. The relationship among c-Myc, GSH content, and the response to alkylating agent has been also evaluated in the M14 Myc overexpressing clones as well as in the melanoma JR8 c-Myc antisense transfectants. All together, these results demonstrate that GSH plays a key role in governing c-Myc–dependent drug-induced apoptosis. *Neoplasia* (2004) 6, 195–206

**Keywords:** c-Myc, glutathione, antineoplastic drugs, apoptosis, melanoma.

## Introduction

Several papers report that susceptibility to apoptosis can contribute to the response of tumor cells to most cytotoxic agents currently used. Thus, alterations that impair susceptibility to apoptosis should produce drug resistance. Muta-

tions affecting the *c-myc* proto-oncogene are among the most common genetic lesions found in a variety of human cancers [1,2]. The role of *c-myc* oncogene on apoptosis has been extensively documented. Under appropriate circumstances, both repression and overexpression of c-Myc can lead to apoptosis. For example, *c-myc* antisense or dominant-defective causes apoptosis in a variety of transformed cell types [3], whereas c-Myc expression can sensitize cells to a wide range of different stimuli such as low serum conditions [4], hypoxia [5], and deprivation of specific growth factors [6,7]. Many studies have been dedicated to c-Myc–mediated apoptotic pathways initiated by DNA-damaging agents due to the potential relevance to cancer chemotherapy. Nevertheless, the role of c-Myc in susceptibility to drug-induced cell death is still obscure with results being contradictory up to now.

Deregulated c-Myc expression has been reported not only to enhance tumor cell sensitivity but also to induce resistance to antineoplastic agents. In particular, overexpression of c-Myc has been reported to increase cellular susceptibility to chemotherapy-induced apoptosis [8–10]. Conversely, in other experimental models, c-Myc overexpression increases the resistance to alkylating agents, as well as to adriamycin (ADR) and etoposide, whereas it does not influence the response to ionizing radiation [11,12]. Then again, inducible antisense *c-myc* gene transfer confers sensitivity to cisplatin (CDDP) in a drug-resistant human small cell lung carcinoma line [13]. In this context, we previously demonstrated that treatment with *c-myc* antisense oligodeoxynucleotides induces apoptosis and enhances CDDP antitumoral efficacy in several human melanoma cell lines [14–16]. The role of c-Myc on the apoptosis and drug sensitivity of melanoma cells has been evaluated by our group by using stable c-Myc low-expressing transfectants. We have demonstrated that although c-Myc downregulation induces apoptosis and sensitizes M14

Abbreviations: ADR, adriamycin; CDDP, cisplatin; L-PAM, melphalan; CPT, camptothecin; ROS, reactive oxygen species;  $\Delta\psi_m$ , mitochondrial membrane potential; DHE, dihydroethidium; GSH, reduced glutathione; BSO, L-buthionine-sulfoximine; PI, propidium iodide; PIPES, piperazine-*N,N'*-bis[2-ethanesulfonic acid]; PBS, phosphate-buffered saline

Address all correspondence to: Dr. Annamaria Biroccio, Experimental Chemotherapy Laboratory, Regina Elena Cancer Institute, Via delle Messi d'Oro 156, Rome 00158, Italy. E-mail: [biroccio@ifo.it](mailto:biroccio@ifo.it)

<sup>1</sup>This work was supported by grants from the Italian Association for Cancer Research (AIRC), Ministero della Salute, and CNR-MIUR.

Received 26 September 2003; Revised 16 December 2003; Accepted 22 December 2003.

melanoma cells to the alkylating agent CDDP, it has no such effect with DNA topoisomerase inhibitors ADR and camptothecin (CPT) [17]. Recently, by using inducible c-Myc antisense transfectants, we also found that down-regulation of c-Myc triggers apoptosis through glutathione (GSH) depletion [18]. GSH is an endogenous cysteine-containing tripeptide, playing a key role in drug detoxification through a number of mechanisms, including antioxidant activity [19], DNA repair [20,21], conjugation of cellular toxins [22], and pumping of toxic chemotherapeutics out of cells through the multidrug resistance–associated proteins [23]. Elevated intracellular GSH can augment cell resistance to irradiation and chemotherapy, especially to alkylating agents, whereas diminution of intracellular GSH content can increase cell response to radiotherapy and chemotherapy [19,24]. Drug resistance has been correlated to increased levels of both messenger RNA and activity of  $\gamma$ -glutamylcysteine synthetase [25,26]—the rate-limiting enzyme for GSH biosynthesis. In addition, transfection of the cDNA encoding for this enzyme into tumor cells leads to increased activity and drug resistance, along with GSH levels [27].

Hence, the main objective of this paper was to investigate the role of GSH on the c-Myc–dependent chemosensitivity of melanoma cells.

## Materials and Methods

### Cell Culture

Three stable c-Myc antisense transfectants (MAS51, MAS53, and MAS69) and a control clone (MN2) were previously obtained by transfecting the M14 human melanoma parental line with an expression vector carrying the antisense *c-myc* cDNA and/or the neomycin selection marker gene [17]. M14 cells were also transfected with the pCDNA1–*c-myc* cDNA expression vector and two c-Myc overexpressing clones (MS41 and MS58) were selected and employed in the study. Moreover, three stable c-Myc antisense transfectants (JAS26, JAS28, and JAS43) and the JN3 control clone were obtained by transfecting the JR8 melanoma cell line with the pCDNA3–*c-myc* antisense expression vector and the empty vector, respectively. All transfectants were grown at 37°C in completed neomycin-containing (0.8 mg/ml; Invitrogen, Carlsbad, CA) RPMI 1640 medium (Invitrogen).

### Treatments

Clinical-grade CDDP (Pronto Platamine) and ADR (Adriablastina) were obtained from Pharmacia (Milan, Italy). CPT and melphalan (L-PAM; Alkeran) were purchased from Sigma (Milan, Italy) and Glaxo Wellcome (Verona, Italy), respectively. Drug dilutions were freshly prepared before each experiment.

In particular, cells were seeded in 60-mm Petri (Nunc, Mascia Brunelli, Milan, Italy) dishes at a density of  $2 \times 10^5$  cells/dish. After 24 hours, cells were exposed to increasing doses of drugs (for clonogenic experiments) or to the  $IC_{50}$

dose of each antineoplastic agent (for all the other assays). The  $IC_{50}$  doses employed were 6.7  $\mu$ M CDDP for 2 hours, 15  $\mu$ M L-PAM for 2 hours, 0.37  $\mu$ M ADR for 1 hour, and 2  $\mu$ M CPT for 2 hours.

To evaluate cell colony-forming ability, aliquots of cell suspension from each sample were seeded into 60-mm Petri dishes with complete medium and incubated for 10 to 12 days. Colonies were stained with 2% methylene blue in 95% ethanol and counted (one colony  $\geq$  50 cells). Surviving fractions were calculated as the ratio of absolute survival of the treated sample/absolute survival of the control sample.

In the experiments with GSH ethyl ester (Sigma) or L-buthionine-sulfoximine (BSO; Sigma), cells were preincubated with 5 mM GSH ethyl ester for 24 hours or with 10 mM BSO for 6 hours (doses with no toxic effect on cell survival). Then cells were washed three-fold and treated with the different antineoplastic agents.

### Evaluation of Apoptosis

Apoptosis was detected by flow cytometric (annexin V), biochemical (caspase-3 activity), and morphological (Hoechst staining) assays. Annexin V-FITC *versus* propidium iodide (PI) assay (Vibrant apoptosis assay, V-13242; Molecular Probes, Eugene, OR) was performed as previously described [18]. Briefly, adherent cells were harvested, suspended in the annexin-binding buffer ( $1 \times 10^6$  cells/ml), and incubated with annexin V-FITC and PI for 15 minutes, at room temperature in the dark, then immediately analyzed by flow cytometry. The data are presented as biparametric dot plots showing the annexin V-FITC green fluorescence *versus* the PI red fluorescence. Analysis of cell death was performed from 0 to 96 hours after the end of each drug treatment.

Caspase-3 activity was measured by a colorimetric assay (K2027; Clontech, Basingstoke, UK) according to the manufacturer's instruction.

Cytopreparations were stained with Hoechst 33258 dye (Sigma) and cover-slipped. Cell morphology was evaluated by fluorescence microscopy.

### GSH Determination

Intracellular GSH content was measured by a colorimetric assay (Bioxytech GSH-400; Oxis International, Inc., Portland, OR) according to the manufacturer's instruction.

### Determination of Cytosolic Proteins

The determination of cytosolic proteins was performed as previously reported [18]. Cells were harvested and washed with phosphate-buffered saline (PBS), then collected by centrifugation at  $700 \times g$  for 7 minutes at 4°C. Cell pellet was resuspended in extraction buffer containing 220 mM mannitol, 68 mM sucrose, 50 mM piperazine-*N,N'*-bis[2-ethanesulfonic acid] (PIPES)–NaOH (pH 7.4), 50 mM EGTA, 2 mM  $MgCl_2$ , 1 mM dithiothreitol, and protease inhibitors. After 30 minutes of incubation on ice, cells were homogenized with glass Dounce homogenizer. Cell homogenates were spun at  $14,000 \times g$  for 15 minutes at 4°C, and

supernatants were removed and stored at  $-80^{\circ}\text{C}$  until analysis by gel electrophoresis. Twenty micrograms of cytosolic protein extracts was run on denaturing 12% sodium dodecyl sulfate polyacrylamide gel electrophoresis. Rabbit anti-procaspase-3 (1:500; Upstate Biotechnology, New York, NY), mouse anti-Bcl-2 (1:200, clone 124; DAKO SA, Glostrup, Denmark), rabbit anti-Bcl-x<sub>L</sub> (1:500, clone S-18; Santa Cruz Biotechnology, Santa Cruz, CA), rabbit anti-Bax (1:500, clone N-20; Santa Cruz Biotechnology), mouse anti-cytochrome *c* (1:500, clone 7H8.2c12; Pharmingen, San Diego, CA), mouse anti-caspase-9 (1:500, clone 96-2-2; Upstate Biotechnology), and mouse anti- $\beta$ -actin, (1:1,000, clone AC-40; Sigma) antibodies were used to detect protein expression in the extramitochondria compartment. Enhanced Chemiluminescence Detection System (ECL) was employed for chemoluminescence detection.

#### Mitochondrial Membrane Potential ( $\Delta\psi_m$ )

$\Delta\psi_m$  was assessed by using JC-1, a cationic dye that exhibits mitochondria potential-dependent accumulation, without being affected by plasmalemma potential. JC-1 accumulates in the cytoplasm, where it produces green fluorescence and forms red fluorescent J-aggregates in the mitochondria. Mitochondria depolarization is indicated by a decrease in the red/green fluorescence intensity ratio. Adherent cells (about  $5 \times 10^5$ ) were first assayed for viability and then loaded with  $10 \mu\text{M}$  JC-1 in RPMI 1640 medium, for 30 minutes at  $37^{\circ}\text{C}$  in the dark. After incubation, cells were washed twice and resuspended in PBS, then immediately analyzed by flow cytometry. As positive control of the assay, M14 cells were treated with increasing doses of either FCCP (0.1, 1, and  $5 \mu\text{M}$  for 10 minutes) or valinomycin (0.01, 0.1, and  $1 \mu\text{g/ml}$  for 10 minutes). As internal negative control, cells were exposed to nigericin (0.1, 1, and  $10 \mu\text{g/ml}$  for 10 minutes). The data are presented as biparametric panels with the green J-monomers fluorescence plotted *versus* the red J-aggregates fluorescence. Analysis of  $\Delta\psi_m$  was performed from 0 to 72 hours following the end of each drug administration.

#### Reactive Oxygen Species (ROS) Production

The evaluation of ROS was performed as previously described [17]. Briefly, adherent cells (about  $5 \times 10^5$ ) were first assayed for viability and then incubated with  $4 \mu\text{M}$  dihydroethidium (DHE; Molecular Probes, Eugene, OR) for 45 minutes at  $37^{\circ}\text{C}$  in PBS. After incubation, cells were immediately analyzed by flow cytometry. The data are presented as biparametric panels with the red DHE fluorescence intensity plotted *versus* the forward scatter. Analysis of ROS generation was performed from 0 to 72 hours following the end of each drug treatment.

#### Statistical Analysis

The results are presented as mean  $\pm$  S.D. Significant changes were assessed by using Student's *t*-test for unpaired data, and *P* values less than .05 were considered significant.

## Results

### *Effects of c-Myc Downregulation on Apoptosis Vary According to Specific Drug Action*

We previously demonstrated that the downregulation of c-Myc increases the susceptibility of M14 melanoma cell line to the alkylating agent CDDP, but not to DNA topoisomerase inhibitors ADR and CPT [17]. In particular, the CDDP dose inhibiting survival by about 50% in control cells ( $6.7 \mu\text{M}$ ) was able to reduce the surviving fraction of c-Myc antisense transfectants by about 90%. By contrast, at  $0.37 \mu\text{M}$  ADR and  $2 \mu\text{M}$  CPT, the survival of both control and c-Myc antisense transfectants was about 50%.

With the aim to study the mechanism(s) responsible for the different drug responses elicited by the reduction of c-Myc expression, three M14-derived clones, expressing low levels of c-Myc (MAS51, MAS53, and MAS69) compared to control cells (M14 parental line and MN2 control clone) previously obtained and characterized [17], were used. Figure 1A shows the cytofluorimetric analysis of the annexin V *versus* PI staining performed in MN2 control clone and in the representative MAS69 c-Myc transfectant. Cells were treated with the IC<sub>50</sub> dose of each antineoplastic agent. Besides ADR ( $0.37 \mu\text{M}$ ), CPT ( $2 \mu\text{M}$ ), and CDDP ( $6.7 \mu\text{M}$ ), another alkylating agent, L-PAM ( $15 \mu\text{M}$ ), was included in the study, and the kinetics of cell death was followed up from 0 to 96 hours after the end of each drug administration. Following treatments with CDDP and L-PAM, no apoptosis (annexin V<sup>+</sup>/PI<sup>-</sup> region of the dot plot panels) was observed in the MN2 control clone, whereas an increasing percentage of the annexin V<sup>+</sup>/PI<sup>+</sup> cells appeared with time after exposure to both alkylating agents. By contrast, c-Myc low-expressing cells were much more susceptible to CDDP- and L-PAM-induced cell death, showing an increasing percentage of apoptotic cells after treatment with both alkylating agents. However, apoptosis was triggered in both MN2 control and c-Myc antisense transfectants by exposure to ADR and also CPT, with the percentage of the annexin V<sup>+</sup>/PI<sup>-</sup> cells increasing from 0 to 96 hours following treatment. Figure 1B shows the percentage of both annexin V<sup>+</sup>/PI<sup>-</sup> and annexin V<sup>+</sup>/PI<sup>+</sup> cells after each drug administration, reported for all the controls and the three c-Myc antisense transfectants. As evident, after CDDP and L-PAM treatments, neither control line had more than 5% of annexin V<sup>+</sup>/PI<sup>-</sup> cells, whereas a progressive significant increase in the annexin V<sup>+</sup>/PI<sup>+</sup> cells (from about 5% to 45%) was observed. On the contrary, c-Myc antisense transfectants showed an increase of both PI<sup>-</sup> and PI<sup>+</sup> annexin V<sup>+</sup> cells following alkylating agent exposure. Then again, all cells, both control and c-Myc low-expressing cells, died prevalently from apoptosis following exposure to topoisomerase inhibitors, with the percentage of the annexin V<sup>+</sup>/PI<sup>-</sup> cells reaching values of about 40% 96 hours after the end of ADR and CPT treatment.

Biochemical and morphological evaluation of cell death was also performed at 96 hours after the end of drug exposure. Figure 2A shows the analysis of caspase-3 activity (upper panels) and the expression of its inactive form



### GSH Depletion Activates Apoptosis on Treatment with Alkylating Agents But Not with Topoisomerase Inhibitors

Because we previously demonstrated that c-Myc downregulation decreases the intracellular GSH content [18], we

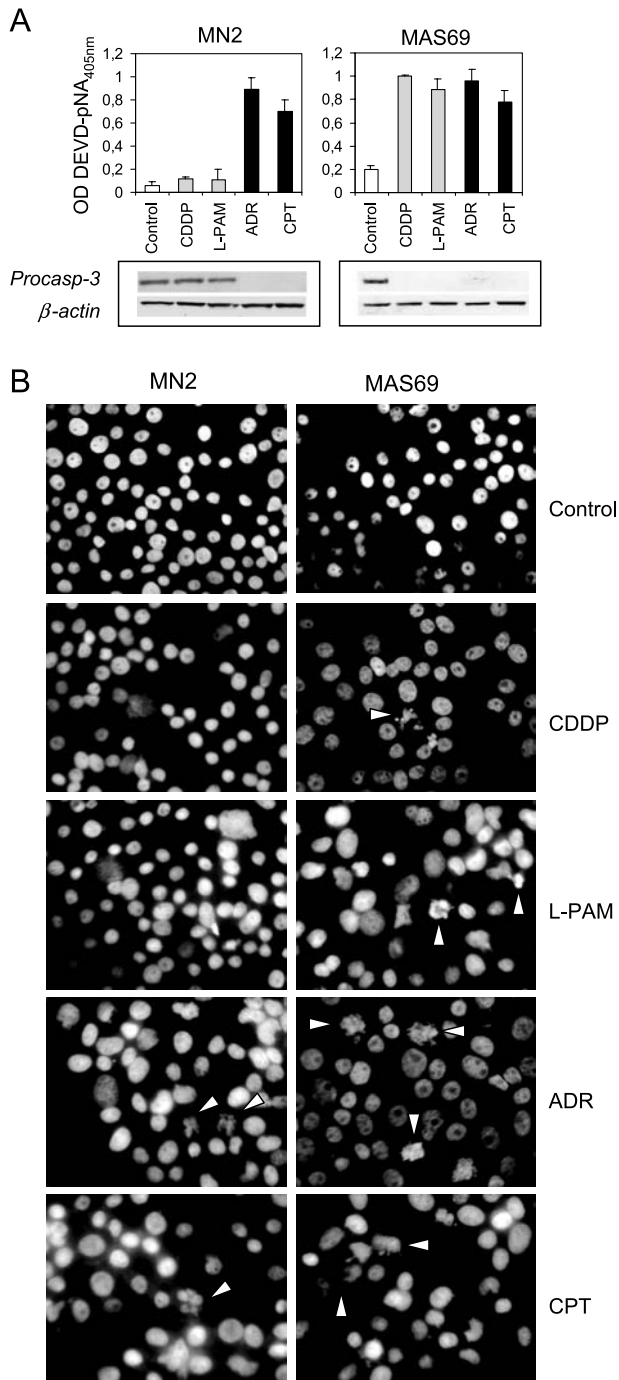


**Figure 2.** c-Myc downregulation opens the apoptotic pathway on treatment with alkylating agents. (A) Evaluation of caspase-3 activity (upper panels,  $P$  values  $< .05$  for MAS69 when compared to MN2 control clone following treatment with alkylating agents) and procaspase-3 expression (bottom panels) performed in the representative MN2 control clone and MAS69 c-Myc transfectant 96 hours after the end of the treatment with the  $IC_{50}$  doses of CDDP, L-PAM, ADR, or CPT. (B) Morphological analysis of cell death performed by Hoechst staining in the representative MN2 control clone and MAS69 c-Myc transfectant 96 hours after the end of the treatment with the  $IC_{50}$  doses of CDDP, L-PAM, ADR, or CPT. White arrows indicate apoptotic cells.

investigated whether it was responsible for the opening of the apoptotic pathway observed in the c-Myc low-expressing clones when treated with the alkylating agents. To this aim, the intracellular GSH concentration was modulated in control cells by incubation with BSO, a specific inhibitor of GSH synthesis. The administration of BSO, given before each drug exposure, depleted intracellular GSH concentration in the control cells by 50% (Figure 3A). Figure 3B (upper panels) shows that the depletion of GSH, achieved by preincubation with BSO, activated apoptosis in M14 and MN2 control cells following treatment with CDDP and L-PAM. Apoptosis was already evident as early as 24 hours and enhanced with increasing time, reaching about 40% at 72 hours, similar to that observed in the c-Myc antisense transfectants. By contrast, when BSO was administered before exposure to ADR and CPT, no change in the drug-mediated apoptosis was observed, with the percentage of the annexin V<sup>+</sup>/PI<sup>-</sup> cells being similar between BSO-preincubated and unincubated control cells (Figure 3B, bottom panels).

The specific role of GSH in the c-Myc–dependent drug-induced apoptosis was demonstrated by increasing the intracellular GSH content in the c-Myc antisense transfectants. Figure 4 shows the intracellular GSH content and apoptosis in the three c-Myc low-expressing clones exposed to GSH ethyl ester. The intracellular GSH content was raised by about two-fold in the c-Myc low-expressing clones on treatment with GSH ethyl ester (Figure 4A). CDDP- and L-PAM–triggered apoptosis was completely abrogated in the c-Myc antisense transfectants when preincubated with GSH ethyl ester because no annexin V<sup>+</sup>/PI<sup>-</sup> cells were observed in the ester-treated c-Myc low-expressing clones within the 72 hours after treatment (Figure 4B, upper panels). On the contrary, the increase in GSH content following ester administration did not protect the c-Myc low-expressing clones from the ADR- and CPT-induced apoptosis (Figure 4B, bottom panels).

To strengthen the relationship among c-Myc, GSH, and drug sensitivity, M14 cells have been transfected with a c-myc cDNA-containing vector and two selected c-Myc overexpressing clones have been used. Figure 5A shows the Western blot analysis of c-Myc protein expression and the corresponding intracellular GSH content evaluated in MN2 control clone, MS41, and MS58 c-Myc transfectants. The amount of c-Myc protein in the two c-Myc overexpressing clones was about two- to three-fold higher than the MN2 control clone, and GSH content was about 50 and 65 nmol/mg protein in the control and c-Myc transfectants, respectively. The enhancement of intracellular GSH content induced by c-Myc overexpression led to an increase in CDDP resistance well evident at the highest dose employed (Figure 5B). In fact, the surviving fractions at 16  $\mu$ M were about 10% in the control clone and about 50% in the two c-Myc transfectants. BSO-mediated GSH depletion in MS41 and MS58 c-Myc transfectants significantly sensitized them to CDDP treatment, with the survival of the c-Myc overexpressing clones being about 1% in the BSO-treated cells at 16  $\mu$ M drug concentration.

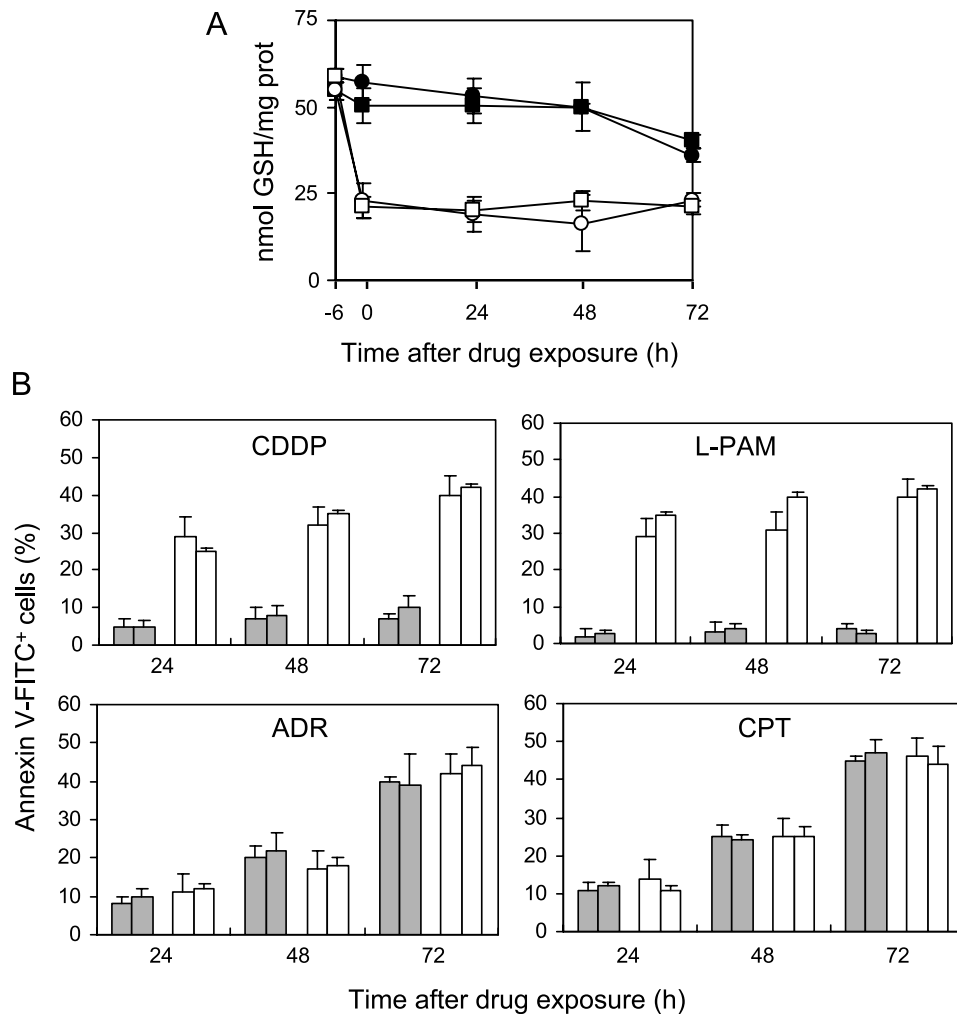


**Figure 3.** GSH depletion achieved by BSO pretreatment commits control cells to alkylating agent-induced apoptosis, without affecting the response to ADR and CPT. (A) Intracellular GSH content evaluated in the untreated M14 (●) and MN2 control (■) cells and BSO-treated M14 (○) and MN2 (□) cells before (–6 hours) and from 0 to 72 hours following exposure to BSO (10 mM; 6 hours). Statistical analysis:  $P < .01$  at 24 to 72 hours after drug exposure for BSO-exposed control cells when compared to unexposed ones. (B) Cytofluorimetric evaluation of apoptotic (annexin V<sup>+</sup>/PI<sup>+</sup>) M14 and MN2 control cells preincubated (white bars) or not (gray bars) with BSO and treated with the  $IC_{50}$  doses of CDDP, L-PAM, ADR, or CPT. Analysis was performed from 24 to 72 hours following the end of the treatments. Control cells, both unexposed and exposed to BSO, did not show any apoptosis; thus, their values have not been included in the histograms. Statistical analysis:  $P < .05$  at 24 hours,  $< .01$  at 48 to 72 hours after exposure to CDDP and L-PAM calculated for BSO-exposed control cells when compared to unexposed ones.

#### Drug-Induced Apoptosis Modulated by GSH through Its Action on Mitochondria Level

To identify the signaling molecules involved in GSH-modulated apoptosis following treatments with CDDP and L-PAM, we analyzed the activation of CD95 receptor pathway, the status of p53, and the role of mitochondria.

GSH-dependent apoptosis did not involve either the CD95 system or any modulation in the p53 protein expression (data not shown). In addition, although the sequencing analysis of the most mutated hot spot regions in the p53-encoding sequence revealed that they were all wild type, the p53 oncoprotein was not active in the M14 melanoma cells (data not shown).

To determine the role of the mitochondria pathway, we checked the cytosolic Bcl-2, Bcl-x<sub>L</sub>, and Bax levels; cytochrome *c*; and the cleavage of procaspase-9. BSO-induced apoptosis in control cells following treatment with alkylating

agents did not involve changes in the expression of Bcl-2 and Bcl-x<sub>L</sub> (Figure 6A). On the contrary, a reduction in the cytosolic Bax expression and a cytochrome *c* redistribution were evident 24 hours after the end of treatment with CDDP and L-PAM in the BSO-exposed control cells. Consequently, procaspase-9 was found to be activated by cleavage exclusively in the BSO-exposed control cells after treatment with both alkylating agents. No modulation of these molecules was observed in the BSO-unexposed control cells when treated with CDDP and L-PAM.

The early Bax/cytochrome *c* translocation observed in BSO-exposed control cells on treatment with CDDP and L-PAM occurred independently of the depolarization of the mitochondria membrane potential. As shown in Figure 6B (upper panels), a significant reduction in  $\Delta\psi_m$  was observed only 48 hours after the end of the treatments with both alkylating agents, whereas no shift in the JC-1 double

fluorescence was revealed in the CDDP- and L-PAM-treated MN2 control clone. Moreover, the alkylator-dependent alteration of  $\Delta\psi_m$  was concomitant to the generation of ROS. Figure 6B (bottom panels) shows that CDDP and L-PAM treatments led to late ROS generation exclusively in the BSO-exposed control cells starting 48 hours after the end of the exposure to both alkylating agents, downstream cytochrome *c* release, and caspase-9 activation. The observed alteration of  $\Delta\psi_m$  and ROS production enhanced with increasing time after drug treatment (data not shown).

The ability of GSH to modulate drug-induced apoptosis by acting at the mitochondria level was also observed when GSH content was increased in the c-Myc low-expressing cells after exposure with GSH ethyl ester. As shown in the Figure 7, the treatment of the c-Myc low-expressing cells with CDDP and L-PAM activated the same mitochondrial pathway: early Bax redistribution, release of cytochrome *c*,

and concomitant caspase-9 activation (Figure 7A), upstream alteration of mitochondria membrane potential (Figure 7B, upper panels), and ROS production (Figure 7B, bottom panels). GSH ester preincubation inhibited the apoptotic cascade by blocking the early apoptotic events. Indeed, Bax and cytochrome *c* redistribution was completely abrogated in the GSH ester-exposed c-Myc low-expressing cells following treatment with both alkylating agents (Figure 7A). Consequently, the downstream mitochondria membrane depolarization and ROS generation were inhibited in the GSH ester-exposed c-Myc antisense transfectant treated with CDDP and L-PAM (Figure 7B).

All the same experiments were performed in the M14 parental line and MAS51 and MAS53 c-Myc low-expressing clones, giving similar results to those obtained with the MN2 and MAS69 c-Myc antisense transfectants (data not shown).

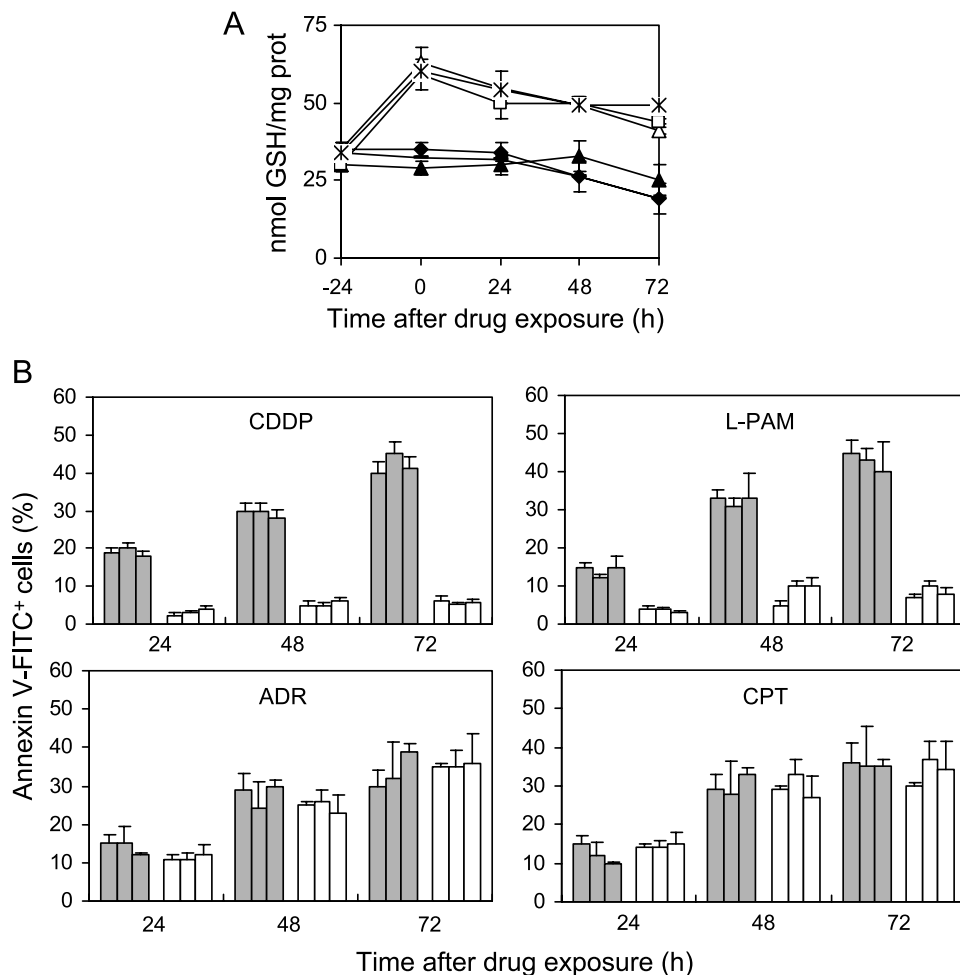


**Figure 4.** GSH increase following ester administration protects c-Myc transfectants from CDDP- and L-PAM-triggered apoptosis, without altering topoisomerase inhibitor-induced cell death. (A) Intracellular GSH content evaluated in the untreated MAS51 (▲), MAS53 (◆), and MAS69 (-) c-Myc transfectants and GSH ester-treated MAS51 (△), MAS53 (◇), and MAS69 (+) c-Myc transfectants before (-24 hours) and from 0 to 72 hours following exposure to GSH ethyl ester (5 mM; 24 hours). Statistical analysis:  $P < .01$  at 24 to 72 hours after drug exposure for GSH ester-exposed c-Myc antisense transfectants when compared to unexposed ones. (B) Cytofluorimetric evaluation of apoptotic (annexin V<sup>+</sup>/PI<sup>-</sup>) MAS51, MAS53, and MAS69 c-Myc low-expressing clones cells preincubated (white bars) or not (gray bars) with GSH ester and treated with the IC<sub>50</sub> doses of CDDP, L-PAM, ADR, or CPT. Analysis was performed from 24 to 72 hours following the end of the treatments. Values for c-Myc transfectants, both unexposed and exposed to GSH ester, are always below 10%; thus, they have not been included in the histograms. Statistical analysis:  $P < .05$  at 24 hours,  $< .01$  at 48 to 72 hours after exposure to CDDP and L-PAM calculated for GSH ester-exposed c-Myc antisense transfectants when compared to unexposed ones.

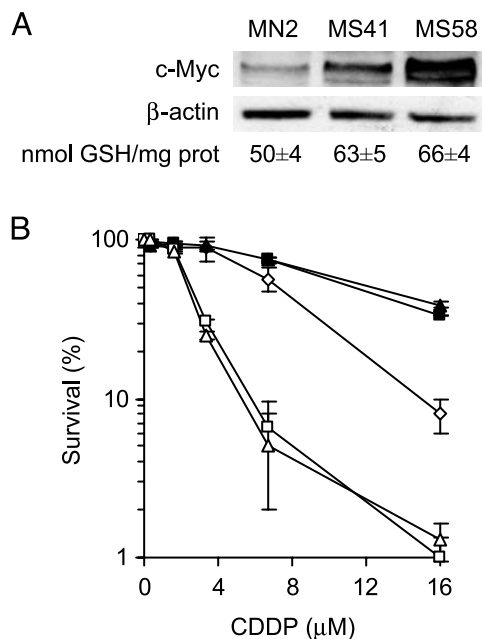


**Figure 5.** *c-Myc*–dependent GSH increase induces resistance to CDDP treatment. (A) Western blot of *c-Myc* protein expression and intracellular GSH content performed in the MN2 control clone and in the MS41 and MS58 *c-Myc* overexpressing clones ( $P < .05$  calculated for all *c-Myc* transfectants when compared to control cells). (B) Survival curves of MN2 control clone (◇), MS41 (■), MS58 (▲) *c-Myc* transfectants, BSO-exposed MS41 (□), and BSO-exposed MS58 (△) treated with increasing doses of CDDP. Surviving fractions were calculated as ratio of the absolute survival of the treated sample/absolute survival of the untreated one ( $P < .01$  calculated for the two *c-Myc* transfectants when compared to control clone at 16 μM CDDP, and  $P < .001$  calculated for unexposed when compared to BSO-exposed *c-Myc* transfectants).

#### Relationship Among *c-Myc*, Intracellular GSH Content, and Alkylating Agent–Induced Apoptosis in JR8 Melanoma Cells

To extend the results obtained, an other human melanoma line, displaying a high level of *c-Myc* protein, was transfected with an expression vector carrying *c-myc* cDNA in antisense orientation. Figure 8A shows the Western blot analysis of *c-Myc* protein expression in JR8 parental line, JN3 control clone, and three *c-Myc* antisense transfectants (JAS26, JAS28, and JAS43). The amount of *c-Myc* protein in the three *c-Myc* antisense transfectants was about five times lower than the JN3 control clone or the parental line. Besides, analysis of intracellular GSH content showed that it was reduced by about 50% in the JAS26, JAS28, and JAS43 *c-Myc* antisense transfectants when compared to control cells (Figure 8B).

To verify the relationship between the *c-Myc*–dependent GSH depletion and drug response, CDDP and ADR were chosen as representative agents for alkylating and topoisomerase inhibitor drugs, respectively. Figure 8C shows the survival curves of the JR8 parental line, the JN3 control clone, and the three *c-Myc* low-expressing clones exposed to increasing doses of CDDP and ADR. *c-Myc* low-expressing clones clearly displayed a greater sensitivity to CDDP if compared to control cells. On the contrary, no difference in sensitivity to ADR among the parental, control, and *c-Myc*

low-expressing cells was observed. Analysis of apoptosis performed by using the  $IC_{50}$  dose of each drug (Figure 8D) demonstrated that CDDP triggered apoptosis in the *c-Myc* antisense transfectants but not in control cells, whereas ADR induced apoptosis in all the lines regardless of *c-Myc* expression. GSH ester pretreatment protected *c-Myc* transfectants from CDDP-induced apoptosis without affecting the ADR-induced cell death.

#### Discussion

In this work, we demonstrate that GSH has a crucial role in the *c-Myc*–dependent drug-induced apoptosis. This paper follows our previous results showing that the downregulation of *c-Myc* sensitizes M14 melanoma cells to alkylating agent CDDP but not to DNA topoisomerase inhibitors ADR and CPT [17]. In an effort to elucidate the mechanism(s) accounting for the different drug sensitivity, we evaluated the ability of drugs to trigger apoptosis, and included another alkylating agent (L-PAM) in the study. Our results demonstrate that both CDDP and L-PAM triggered apoptosis in the *c-Myc* low-expressing clones but not in control lines. On the contrary, activation of programmed cell death occurred to the same extent in control and *c-Myc* antisense transfectants after ADR and CPT administration. Thus, alkylating agents activate a *c-Myc*–dependent apoptosis, whereas a *c-Myc*–independent cell death is induced by topoisomerase inhibitors.

Because we previously demonstrated that *c-Myc* downregulation reduced the intracellular GSH content [18], we hypothesized that GSH might influence the *c-Myc*–dependent (rather than *c-Myc*–independent) drug-induced apoptosis. To this aim, intracellular GSH content was normalized between control and *c-Myc* low-expressing cells. As a result, modulation of GSH content did not affect the response to ADR and CPT, whereas it significantly influenced CDDP- and L-PAM–induced apoptosis. In particular, GSH ester administration in the *c-Myc* low-expressing cells increased the intracellular GSH up to the levels of control cells and abrogated apoptosis induced by CDDP and L-PAM. GSH depletion by BSO preincubation opened the apoptotic pathway in control cells treated with one alkylating agent or the others. The opening of the apoptotic pathway by GSH depletion exclusively occurred following alkylating agents, thus indicating that it was related to the specific drug action.

The relationship among *c-Myc*, GSH content, and the response to alkylating agents has been also evaluated in the M14 *c-Myc* overexpressing clones as well as in the melanoma JR8 *c-Myc* antisense transfectants. The results demonstrated that GSH depletion is responsible for the *c-Myc*–dependent (rather than *c-Myc*–independent) drug-induced apoptosis.

Unlike many other proposed mechanisms of drug resistance, elevated GSH content may act through different pathways to limit the effectiveness of multiple types of chemotherapeutic agents. GSH has been shown to protect tumor cells by detoxifying chemotherapeutic drugs through conjugation reactions catalyzed by GSH S-transferase. Export of GSH conjugate out of tumor

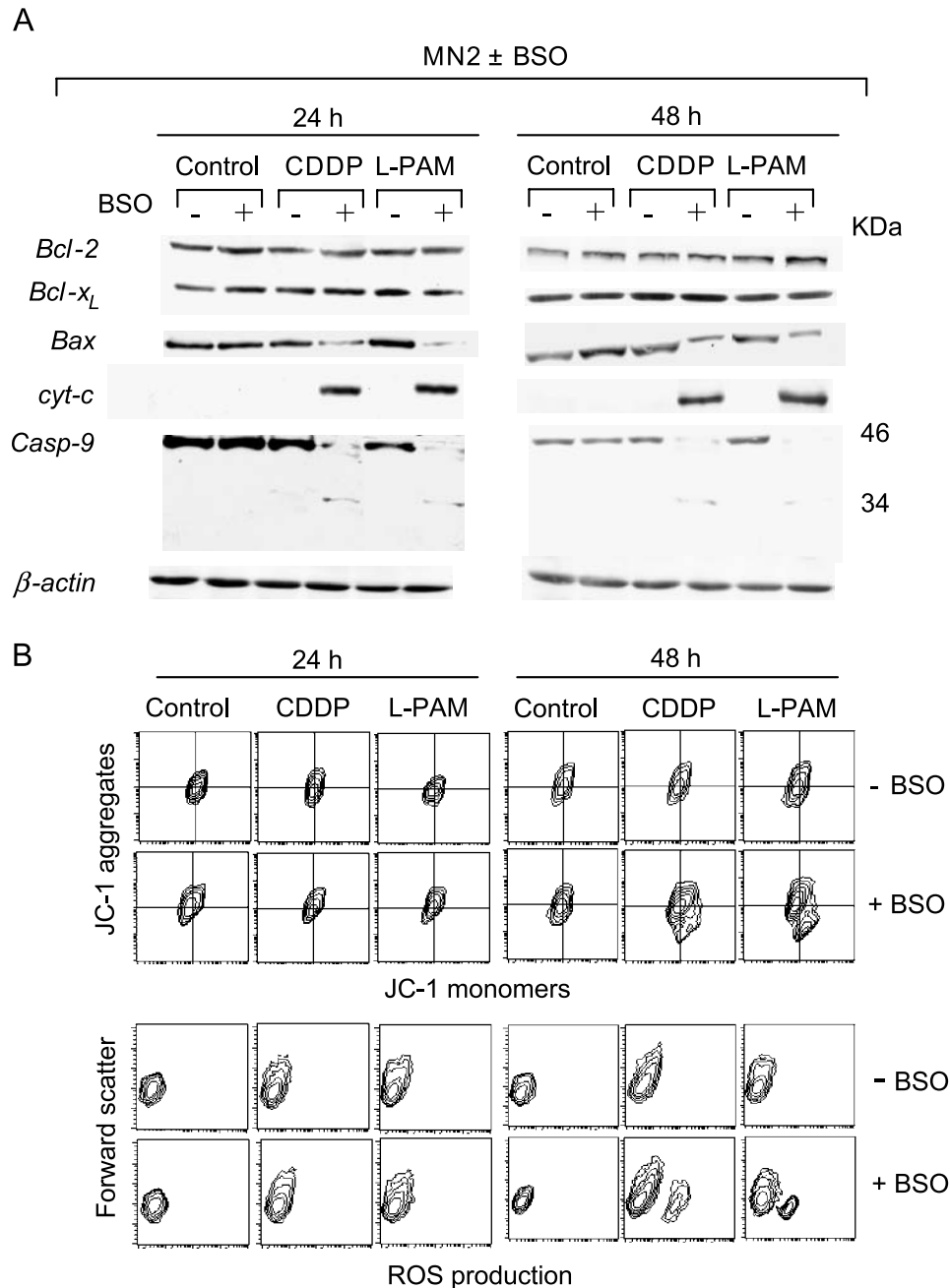


**Figure 6.** BSO-mediated GSH depletion activates the mitochondrial pathway. (A) Immunoblot analysis of cytosolic *Bcl-2*, *Bcl-x<sub>L</sub>*, *Bax*, cytochrome *c*, procaspase-9, and  $\beta$ -actin and (B) cytofluorimetric evaluation of  $\Delta\psi_m$ , evaluated by JC-1 staining (upper panel), and ROS production, carried out by DHE probing (bottom panel), performed in both unexposed and BSO-exposed MN2 control clone 24 and 48 hours following the end of the treatments with the  $IC_{50}$  doses of CDDP and L-PAM. Each panel is representative of four separate experiments with comparable results.

cells by the GS-X pump represents the final elimination of the overall detoxification system [28,29]. In addition, GSH can be transported to the mitochondria, where it plays a protective role as ROS scavenger [30]. The role of GSH or GSH-related mechanisms has been found to be particularly important in the case of alkylating agents [31–33]. In fact, although the GSH-related mechanisms are the most important events in the modulation of cytotoxicity to CDDP and L-PAM, the mechanism for ADR or CPT resistance involves other molecules, such as the P170 in the case of ADR resistance. Moreover,

although the toxicity of CDDP and L-PAM largely depends on intracellular GSH levels, modulation of GSH does not always influence ADR or CPT cytotoxicity, although this does vary among cell types. Depletion of GSH, by prolonged incubation with BSO, increases the lethality of CPT-11 in V79 hamster lung fibroblasts [34], of etoposide in K562 human erythroleukemia cells [35], and of ADR in different cell types [36–38]. In U937 human promonocytic cells, although BSO potentiated the toxicity of CDDP and L-PAM manifested by the suppression of apoptosis and the induction of necrosis, it did not affect the

mode nor the extent of death caused by CPT and ADR. Comprehensively, the literature shows, however, that the key role of GSH content in the sensitivity/resistance to alkylating agents was mainly due to its detoxification or antioxidant properties.

In our experimental models, we can exclude the antioxidant mechanism of GSH as the principal determinant factor in c-Myc–dependent drug sensitivity because we found the ROS production to be not the primary event in the activation of GSH-mediated programmed cell death, but it represents a downstream effector of apoptosis. Here, we show that GSH influenced the c-Myc–dependent alkylator-induced

apoptosis by its ability to act at the mitochondria level, without affecting the p53 and CD95 systems. Instead, BSO-mediated GSH depletion in control cells treated with CDDP and L-PAM rapidly induced Bax/cytochrome *c* redistribution and caspase-9 activation as early events, with alteration of mitochondria membrane potential and ROS production as late events. GSH ester preincubation inhibited the apoptotic cascade by blocking the early and, consequently, the late mitochondria-related apoptotic events. The effect of GSH on the activation of cytochrome *c*–dependent apoptotic pathway might be due to the ability of alkylating agents to bind to GSH [39,40]. This would imply an

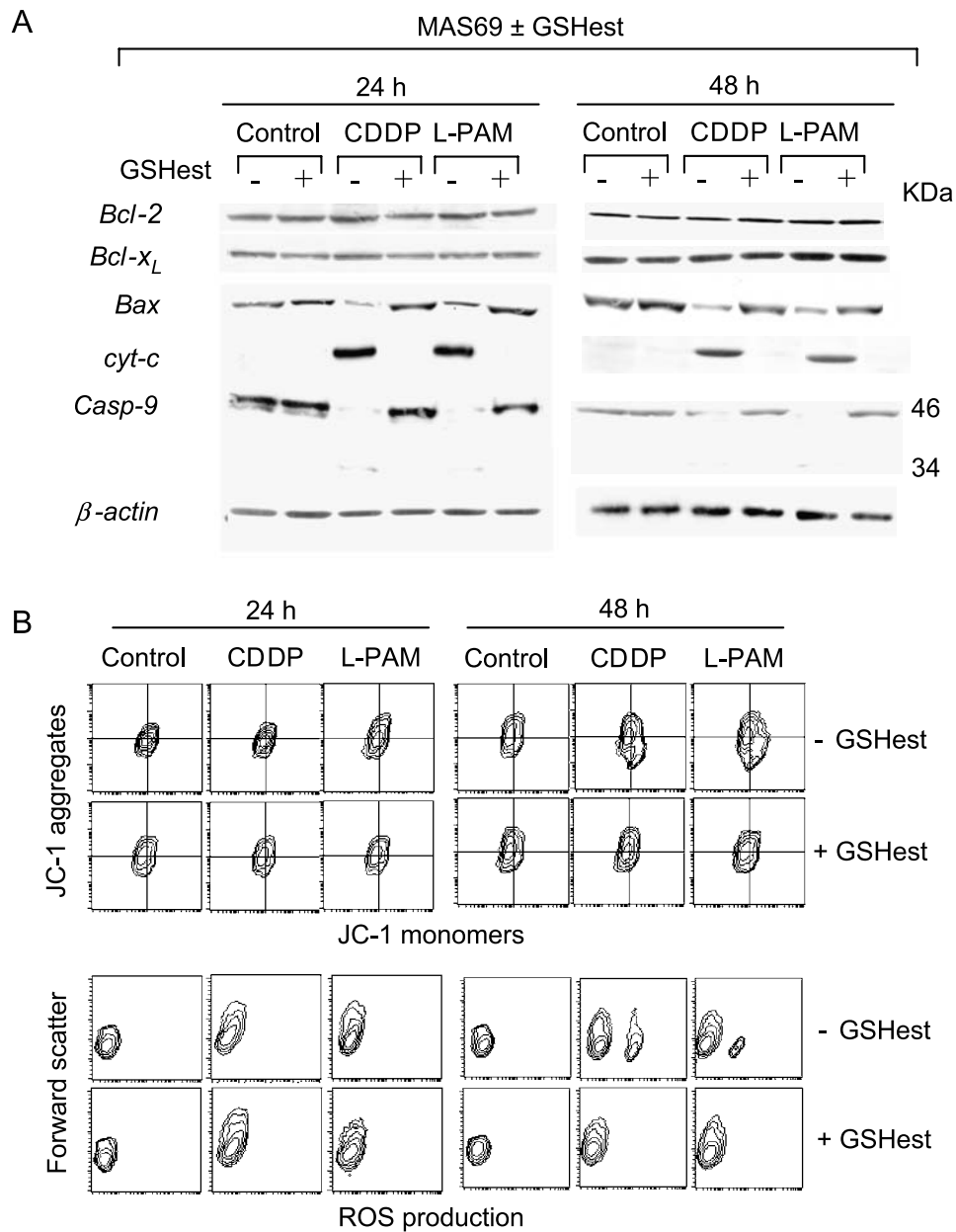


**Figure 7.** Ester-mediated GSH increase inhibits the mitochondrial pathway. (A) Immunoblot analysis of cytosolic *Bcl-2*, *Bcl-x<sub>L</sub>*, *Bax*, cytochrome *c*, procaspase-9, and *β-actin* and (B) cytofluorimetric evaluation of  $\Delta\psi_m$ , evaluated by JC-1 staining (upper panel), and ROS production, carried out by DHE probing (bottom panel), performed in both unexposed and GSH ester-exposed MAS69 c-Myc low-expressing transfectant 24 and 48 hours following the end of the treatments with the IC<sub>50</sub> doses of CDDP and L-PAM. Each panel is representative of four separate experiments with comparable results.

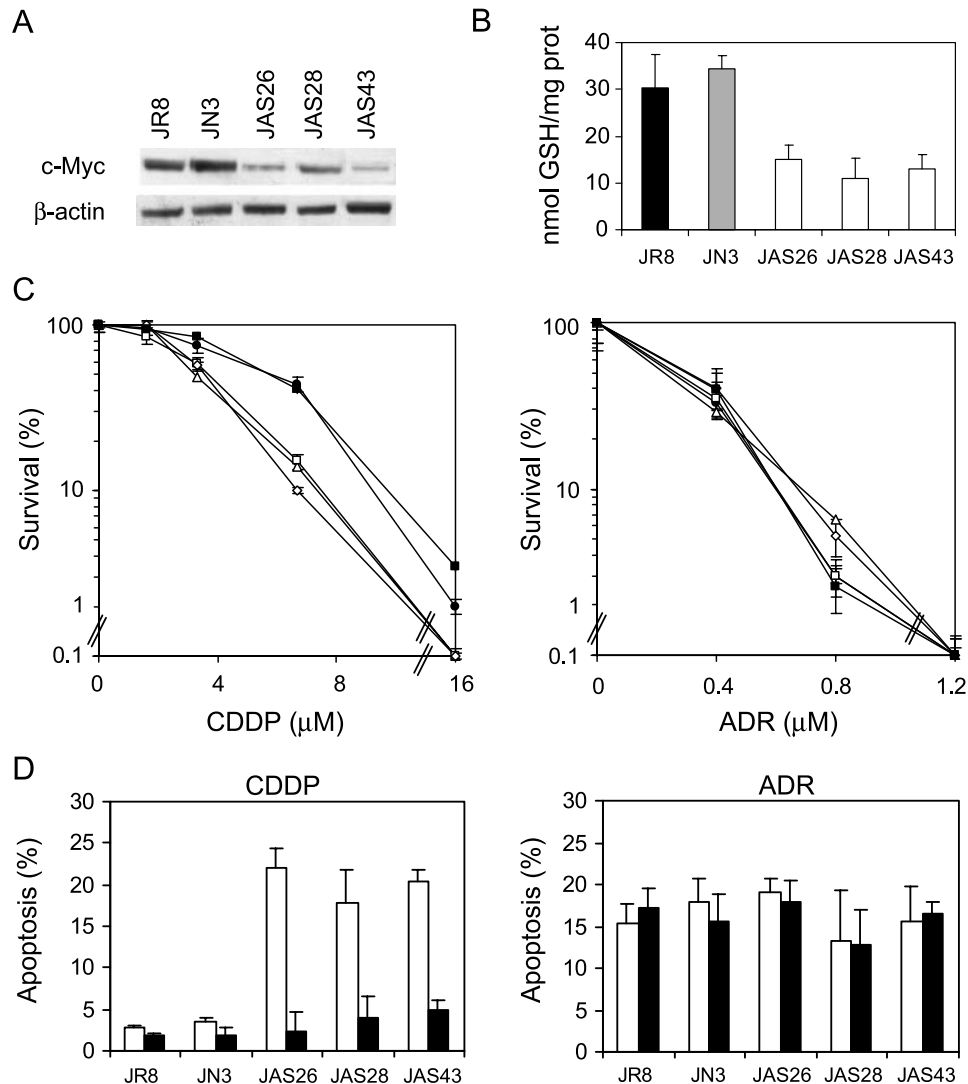


**Figure 8.** Relationship among c-Myc, intracellular GSH content, and alkylating agent–induced apoptosis in the JR8 melanoma cells. (A) Western blot of c-Myc protein expression and (B) intracellular GSH content performed in the JR8 melanoma cell line, JN3 control clone, and JAS26, JAS28, and JAS43 c-Myc low-expressing clones ( $P < .05$  calculated for all c-Myc antisense transfectants when compared to both control cells). (C) Survival curves of JR8 (●), JN3 control clone (■), JAS26 (□), JAS28 (◇), and JAS43 (△) c-Myc antisense transfectants exposed to increasing doses of either CDDP (left panel,  $P < .05$  at 3.4 and  $P < .01$  at 6.7 and 16  $\mu\text{M}$ , calculated for all c-Myc antisense transfectants when compared to both control cells) or ADR (right panel). Surviving fractions were calculated as the ratio of the absolute survival of the treated sample/absolute survival of the untreated one. (D) Percentage of apoptotic cells evaluated 48 hours following the treatment with the  $\text{IC}_{50}$  doses of either CDDP ( $P < .01$  calculated for all c-Myc antisense transfectants when compared to both control cells) or ADR, in both the unexposed (white bars) and GSH ethyl ester–exposed (black bars) JR8 parental line and JN3, JAS26, JAS28, and JAS43 transfectants.

impoverishment of free GSH from the mitochondrial buffer of cells, leading to a cytochrome *c*–dependent apoptosis. Therefore, because we previously demonstrated that c-Myc downregulation decreases GSH content by reducing its synthesis [18], the synergistic effect between c-Myc downregulation and alkylating agents can be attributable to cooperation in the GSH depletion.

In summary, we demonstrate that: 1) alkylating agents trigger a c-Myc–dependent apoptosis, whereas a c-Myc–independent cell death is induced by topoisomerase inhibitors; 2) c-Myc–dependent drug-induced apoptosis is due to GSH depletion; and 3) GSH-mediated drug-induced apoptosis occurs by cytochrome *c* release.

All together, these results lend support to the clinical approach based on c-myc antisense therapy being com-

bined with some antineoplastic agents (i.e., CDDP and L-PAM), rather than others (ADR and CPT).

#### Acknowledgement

We thank Adele Petricca for her helpful assistance in typing the manuscript.

#### References

- [1] Boxer LM and Dang CV (2001). Translocations involving c-myc and c-myc function. *Oncogene* **20**, 5595–5610.
- [2] Nesbit CE, Tersak JM, and Prochownik EV (1999). Myc oncogenes and human neoplastic disease. *Oncogene* **18**, 3004–3016.
- [3] Thompson EB (1998). The many roles of c-Myc in apoptosis. *Annu Rev Physiol* **60**, 575–600.

- [4] Evan GI, Wyllie AH, Gilbert CS, Littlewood TD, Land H, Brooks M, Waters CM, Penn LZ, and Hancock DC (1992). Induction of apoptosis in fibroblasts by c-myc protein. *Cell* **69**, 119–128.
- [5] Alarcon RM, Rupnow BA, Graeber TG, Knox SJ, and Giaccia AJ (1996). Modulation of c-Myc activity and apoptosis *in vivo*. *Cancer Res* **56**, 4315–4319.
- [6] Askew DS, Ashmun RA, Simmons BC, and Cleveland JL (1991). Constitutive c-myc expression in an IL-3–dependent myeloid cell line suppresses cell cycle arrest and accelerates apoptosis. *Oncogene* **6**, 1915–1922.
- [7] Klefstrom J, Vastrik I, Saksela E, Valle J, Eilers M, and Alitalo K (1994). c-Myc induces cellular susceptibility to the cytotoxic action of TNF- $\alpha$ . *EMBO J* **13**, 5442–5450.
- [8] Nesbit CE, Fan S, Zhang H, and Prochownik EV (1998a). Distinct apoptotic responses imparted by c-myc and max. *Blood* **92**, 1003–1010.
- [9] Nesbit CE, Grove LE, Yin XY, and Prochownik EV (1998b). Differential apoptotic behaviors of c-myc, N-myc, and L-myc oncoproteins. *Cell Growth Differ* **9**, 731–741.
- [10] Arango D, Corner GA, Wadler S, Catalano PJ, and Augenlicht LH (2001). c-myc/p53 interaction determines sensitivity of human colon carcinoma cells to 5-fluorouracil *in vitro* and *in vivo*. *Cancer Res* **61**, 4910–4915.
- [11] Sklar MD and Prochownik EV (1991). Modulation of cis-platinum resistance in Friend erythroleukemia cells by c-myc. *Cancer Res* **51**, 2118–2123.
- [12] Niimi S, Nakagawa K, Yokota J, Tsunokawa Y, Nishio K, Terashima Y, Shibuya M, Terada M, and Saijo N (1991). Resistance to anticancer drugs in NIH3T3 cells transfected with c-myc and/or c-H-ras genes. *Br J Cancer* **63**, 237–241.
- [13] Van Waardenburg RC, Meijer C, Burger H, Nooter K, De Vries EG, Mulder NH, and De Jong S (1997). Effects of an inducible anti-sense c-myc gene transfer in a drug-resistant human small-cell-lung-carcinoma cell line. *Int J Cancer* **73**, 544–550.
- [14] Leonetti C, D'Agnano I, Lozupone F, Valentini A, Geiger T, Zon G, Calabretta B, Citro G, and Zupi G (1996). Antitumor effect of c-myc antisense phosphorothioate oligodeoxynucleotides on human melanoma cells *in vitro* and *in vivo*. *J Natl Cancer Inst* **88**, 419–429.
- [15] Citro G, D'Agnano I, Leonetti C, Perini R, Bucci B, Zon G, Calabretta B, and Zupi G (1998). c-myc antisense oligodeoxynucleotides enhance the efficacy of cisplatin in melanoma chemotherapy *in vitro* and in nude mice. *Cancer Res* **58**, 283–289.
- [16] Leonetti C, Biroccio A, Candiloro A, Citro G, Fornari C, Mottolese M, Del Bufalo D, and Zupi G (1999). Increase of cisplatin sensitivity by c-myc antisense oligodeoxynucleotides in a human metastatic melanoma inherently resistant to cisplatin. *Clin Cancer Res* **5**, 2588–2595.
- [17] Biroccio A, Benassi B, Amodei S, Gabellini C, Del Bufalo D, and Zupi G (2001). c-Myc down-regulation increases susceptibility to cisplatin through reactive oxygen species-mediated apoptosis in M14 human melanoma cells. *Mol Pharmacol* **60**, 174–182.
- [18] Biroccio A, Benassi B, Filomeni G, Amodei S, Marchini S, Chiorino G, Rotilio G, Zupi G, and Ciriolo MR (2002). Glutathione influences c-Myc–induced apoptosis in M14 human melanoma cells. *J Biol Chem* **277**, 43763–43770.
- [19] Zhang K, Mack P, and Wong KP (1998). Glutathione-related mechanisms in cellular resistance to anticancer drugs. *Int J Oncol* **12**, 871–882.
- [20] Chen G and Zeller WJ (1991). Augmentation of cisplatin (DDP) cytotoxicity *in vivo* by DL-buthionine sulfoximine (BSO) in DDP-sensitive and -resistant rat ovarian tumors and its relation to DNA interstrand cross links. *Anticancer Res* **11**, 2231–2237.
- [21] Yen L, Woo A, Christopoulos G, Batist G, Panasci L, Roy R, Mitra S, and Alaoui-Jamali MA (1995). Enhanced host cell reactivation capacity and expression of DNA repair genes in human breast cancer cells resistant to bi-functional alkylating agents. *Mutat Res* **337**, 179–189.
- [22] Gamcsik MP, Millis KK, and Hamill TG (1997). Kinetics of the conjugation of aniline mustards with glutathione and thiosulfate. *Chem Biol Interact* **105**, 35–52.
- [23] Barrand MA, Bagrij T, and Neo SY (1997). Multidrug resistance-associated protein: a protein distinct from P-glycoprotein involved in cytotoxic drug expulsion. *Gen Pharmacol* **28**, 639–645.
- [24] Vukovic L and Osmak M (1999). Reversal of carboplatin resistance in human laryngeal carcinoma cells. *Neoplasia* **46**, 335–341.
- [25] Bailey HH, Gipp JJ, Ripple M, Wilding G, and Mulcahy RT (1992). Increase in gamma-glutamylcysteine synthetase activity and steady-state messenger RNA levels in melphalan-resistant DU-145 human prostate carcinoma cells expressing elevated glutathione levels. *Cancer Res* **52**, 5115–5118.
- [26] Godwin AK, Meister A, O'Dwyer PJ, Huang CS, Hamilton TC, and Anderson ME (1992). High resistance to cisplatin in human ovarian cancer cell lines is associated with marked increase of glutathione synthesis. *Proc Natl Acad Sci USA* **89**, 3070–3074.
- [27] Mulcahy RT, Bailey HH, and Gipp JJ (1995). Transfection of complementary DNAs for the heavy and light subunits of human gamma-glutamylcysteine synthetase results in an elevation of intracellular glutathione and resistance to melphalan. *Cancer Res* **55**, 4771–4775.
- [28] Ishikawa T (1992). The ATP-dependent glutathione S-conjugate export pump. *Trends Biochem Sci* **17**, 463–468.
- [29] Ishikawa T and Ali-Osman F (1993). Glutathione-associated cis-diamminedichloroplatinum(II) metabolism and ATP-dependent efflux from leukemia cells. Molecular characterization of glutathione–platinum complex and its biological significance. *J Biol Chem* **268**, 20116–20125.
- [30] Meister A (1991). Glutathione deficiency produced by inhibition of its synthesis, and its reversal; applications in research and therapy. *Pharmacol Ther* **51**, 155–194.
- [31] Meijer C, Mulder NH, Timmer-Bosscha H, Sluiter WJ, Meersma GJ, and de Vries EG (1992). Relationship of cellular glutathione to the cytotoxicity and resistance of seven platinum compounds. *Cancer Res* **52**, 6885–6889.
- [32] Timmer-Bosscha H, Timmer A, Meijer C, de Vries EG, de Jong B, Oosterhuis JW, and Mulder NH (1993). cis-Diamminedichloroplatinum(II) resistance *in vitro* and *in vivo* in human embryonal carcinoma cells. *Cancer Res* **53**, 5707–5713.
- [33] Hamilton D, Fotouhi-Ardakani N, and Batist G (2002). The glutathione system in alkylator resistance. *Cancer Treat Res* **112**, 67–87.
- [34] Sawyer TE and Bonner JA (1996). The interaction of buthionine sulfoximine (BSO) and the topoisomerase I inhibitor CPT-11. *Br J Cancer Suppl* **27**, S109–S113.
- [35] Gantchev TG and Hunting DJ (1997). Enhancement of etoposide (VP-16) cytotoxicity by enzymatic and photodynamically induced oxidative stress. *Anticancer Drugs* **8**, 164–173.
- [36] Lee FY, Vessey AR, and Siemann DW (1988). Glutathione as a determinant of cellular response to doxorubicin. *NCI Monogr* **6**, 211–215.
- [37] Mans DR, Schuurhuis GJ, Treskes M, Lafleur MV, Retel J, Pinedo HM, and Lankelma J (1992). Modulation by DL-buthionine-S,R-sulfoximine of etoposide cytotoxicity on human non-small cell lung, ovarian and breast carcinoma cell lines. *Eur J Cancer* **28A**, 1447–1452.
- [38] Crescimanno M, Borsellino N, Leonardi V, Flandina C, Flugy A, Rausa L, and D'Alessandro N (1994). Effect of buthionine sulfoximine on the sensitivity to doxorubicin of parent and MDR tumor cell lines. *J Chemother* **6**, 343–348.
- [39] Dirven HA, Dictus EL, Broeders NL, van Ommen B, and van Bladeren PJ (1995). The role of human glutathione S-transferase isoenzymes in the formation of glutathione conjugates of the alkylating cytostatic drug thiotepa. *Cancer Res* **55**, 1701–1706.
- [40] David-Cordonnier MH, Laine W, Joubert A, Tardy C, Goossens JF, Kouach M, Briand G, Thi Mai HD, Michel S, Tillequin F, Koch M, Leonce S, Pierre A, and Bailly C (2003). Covalent binding to glutathione of the DNA-alkylating antitumor agent, S23906-1. *Eur J Biochem* **270**, 2848–2859.